ELSEVIER

Biophysical Chemistry 52 (1994) 165–172

Biophysical Chemistry

Influence of vesicle curvature on fluorescence relaxation kinetics of fluorophores

M. Hof [c,*], R. Hutterer [a], N. Pérez [b], H. Ruf [b], F.W. Schneider [a]

[a] *Institute of Physical Chemistry, University of Würzburg, D-97070 Würzburg, Marcusstr. 9/11, Germany*

[b] *Max-Planck Institute for Biophysics, Frankfurt/Main, D-60596 Frankfurt/Main, Kennedy Allee 70, Germany*

[c] *Department of Physical Chemistry, Charles University, 128 40 Prague 2, Albertov 2030, Czech Republic*

Received 17 March 1994; accepted in revised form 26 May 1994

Abstract

The effect of membrane curvature on the fluorescence decay of 2-*p*-toluidinyl-naphthalene-6-sulfonic acid (TNS), 2-(9-anthroyloxy)stearic acid (2-AS) and 12-(9-anthroyloxy)-stearic acid (12-AS) was investigated for egg lecithin vesicles of average diameter $d_m = 22$ nm and 250 nm. The biexponential fluorescence decay of TNS at the red edge of the emission spectrum was analysed according to the model of Gonzalo and Montoro [1]. Over the entire temperature range (1–40°C) the small TNS labelled vesicles showed significantly shorter solvent relaxation times τ_r than their larger counterparts (e.g. 1.3 ns compared with 2.1 ns at 5°C), indicating a higher mobility of the hydrated headgroups in the highly curved, small vesicles. The fluorescence decay of both AS derivatives is also biexponential. While the shorter decay times (1–3 ns) are practically identical for small and large vesicles, the longer decay times (5–14 ns) are identical only for 12-AS but not for 2-AS. This indicates that the microenvironment is similar in small and large vesicles deep in the membrane in spite of the differences in curvature.

Keywords: Time-resolved fluorescence; Membrane curvature; Solvent relaxation; Dynamic light scattering

1. Introduction

The fluorescence decay behaviour of several fluorophores, for example diphenylhexatriene (DPH) [2,3], 1-[4-(trimethylamino)phenyl]-6-phenylhexa-1,3,5-triene (TMA-DPH) [4–6], *n*-(9-anthroyloxy)stearic acids (*n*-AS) [7,8], parinaric acid [9], anthracene [10], 2-*p*-toluidinylnaphthalene-6-sulfonic acid (TNS) [11–13] and 6-palmitoyl-2-[[2-(trimethylammonium)-ethyl]methylamino]-naphthalene chloride (PATMAN) [14,15], in model membranes has been intensively studied. It is generally accepted that the lifetimes of defined localized fluorophores depend on the properties of the membrane microenvironment such as polarity, lipid packing and lipid fluidity. Apart from temperature, composition of the vesicles and pH-value [16] of the aqueous medium the lipid properties and therefore the fluorescence lifetimes may be affected by the curvature of the membrane [3,17]. Only few investigations exist on the influence of membrane curvature on structural parameters of membranes. Several membrane processes, however, are known which are influenced by membrane curvature, for example membrane binding of proteins [18–20], production of thrombin [21] or membrane fusion [22].

With curvature sensitive probes, the curvature dependence of the above listed processes may be inves-

* Corresponding author.

0301-4622/94/$07.00 © 1994 Elsevier Science B.V. All rights reserved
SSDI 0301-4622(94)00093-Y

tigated using fluorescence spectroscopy. The influence of the vesicle size on the membrane structure is illustrated by the fact that the ratio of inner to outer surface increases from about 0.5 for vesicles with a diameter of 20 nm (small unilamellar vesicles, SUV) to nearly unity for vesicles larger than 200 nm. Therefore differences in packing densities between SUV and large, planar bilayers have been suggested [23], but not fully established yet.

Regarding the fluorescence lifetimes in membranes the above mentioned fluorophores can be divided into two categories. The lifetime values of hydrophobic dyes, such as DPH, TMA-DPH, *n*-AS, parinaric acid and anthracene are determined by the quenching processes due to the microenvironment. On the other hand, fluorophores with strongly differing excited and ground state dipole moments, such as TNS, exhibit solvent relaxation and therefore altered fluorescence decay kinetics. The quantitative analysis of these solvent reorientation processes yields information on the mobility of the fluorophore environment. This can be obtained either by analysis of the decay behaviour at a single wavelength [1,24,25] or by the autocorrelation function of the time-dependent red-shift of the fluorescence spectra [11–13,26]. The solvent reorientation monitored by TNS adsorbed to the headgroup region of unilamellar vesicles occurs on the nanosecond timescale and can therefore be detected by single photon counting. The term 'solvent' includes both the hydrated lipid headgroups and those solvent molecules differing from the 'bulk-solvent'.

In the present work the fluorescence decay of variously localized fluorophores in vesicles with a defined size distribution was measured. The quenching by the microenvironment of the backbone region was monitored using 2-AS and 12-AS, and the mobility of the hydrated phospholipid headgroups by TNS. The mobility of the TNS microenvironment was characterized by an average solvent relaxation time τ_r. τ_r represents the average reorientation time necessary to reach a partially solvent relaxed state R of the fluorophore. R covers the ensemble of partially relaxed states from which the emission at a given wavelength λ takes place. If the observed wavelength is at the extreme red end of the fluorescence spectrum, it corresponds to the emission from an almost completely solvent relaxed state R.

In this case, the expression for the fluorescence decay at a temperature T observed at λ simplifies to the difference between two exponential terms [1]

$$f_{T,\lambda} = A \exp[-t/\tau_R] - B \exp[-(1/\tau_R + 1/\tau_r)t] , \quad (1)$$

where τ_R is the decay time of the completely relaxed state R.

Egg lecithin vesicles of two different sizes were prepared using the methods of Brunner et al. [27] and Mimms et al. [28]. The size distribution was determined by dynamic light scattering.

2. Experimental

2.1. Materials

Phosphatidylcholine (PC) was isolated and purified from fresh egg yolks in accordance with Singleton et al. [29]. The purity of the preparation was checked by thin-layer chromatography with a pre-coated silica gel 60F-254 (Merck). Piperazine-1,4-bis(2-ethane sulfonic acid) (Pipes), *n*-octyl-β-D-glucopyranoside and 2-*p*-toluidinylnaphthalene-6-sulfonic acid (TNS) were purchased from Fluka, sodium cholate and all other chemicals from Merck. 2-(9-anthroyloxy)stearic acid (2-AS) and 12-(9-anthroyloxy)stearic acid (12-AS) were obtained from Molecular Probes.

2.2. Preparation of vesicles

Preparation of vesicles using n-octyl-β-D-glucopyranoside and dialysis

Vesicles were prepared according to Mimms et al. [28]. A solution of 50 mg phosphatidylcholine in 1.25 ml methanol was dried to a thin film under nitrogen at about 30°C and remaining traces of solvent removed under vacuum. The lipid film was allowed to swell in 5 ml buffer (65 mM NaCl in 20 mM 'Pipes'-NaOH, pH 7.2) for 1 h at room temperature under nitrogen with gentle shaking and then subjected to a freeze–thaw cycle five times using liquid nitrogen and a water bath set at 40°C in order to facilitate swelling [30]. Then 190 mg *n*-octyl-β-D-glucopyranoside were added to the milky dispersion which turned clear immediately. The molar ratio of detergent to lipid was 10 : 1.

Dialysis was carried out using the same buffer as before at 4°C for 2 days (diameter of dialysis tube = 14.6 mm; Spectrapor). The buffer, presaturated with nitrogen, was changed every 12 h. After dialysis, the vesicle preparation was filtered using a 0.8 mm polycarbonate filter (Nuclepore) and kept at 4°C in a sealed bottle.

Preparation of vesicles using sodium cholate by gel filtration

Egg lecithin dispersions were prepared from a solution of 174 mg phosphatidylcholine in 3.75 ml methanol and allowed to swell in 5.8 ml buffer, as previously. Vesicles were then obtained using the method of Brunner et al. [27]. After addition of 210 mg sodium cholate, dispersions were subjected to a freeze–thaw cycle as before until a clear solution was obtained. Gel filtration was then carried out on a lipid-saturated Sephadex G-50 (medium) column ($h = 25$ cm, diameter = 1.5 cm) which was equilibrated and eluted with the same buffer as before at 4°C and a flow rate of 20 ml/h. In order to remove the remaining cholate an additional 12 h dialysis was carried out using the same buffer as in the column chromatography at 4°C. The vesicle preparation was then filtered and stored. Lipid concentrations were determined by assaying the phosphorus content according to the method of Bartlett [31]. The lipid concentrations of small and large vesicles of the samples used for dynamic light scattering measurements were 7.3 mM and 0.5 mM, respectively.

2.3. Dynamic light scattering

The experimental setup, data collection and data analysis were as described in [32], except that the thermostating bath contained distilled water instead of toluene. The experimental photocount autocorrelation functions consisted of 136 data points equidistant in the delay time, the first three of which were omitted from data analysis to avoid errors due to afterpulsing. In the case of the small vesicles from gel filtration 225 measurements were carried out taking 9×10^7 samples for each employing a sample time per channel of 2 μs. Each measurement was normalized by the baseline value calculated from the total number of photocounts, and the normalized data sets were then averaged. This yielded experimental data from 2.025×10^{10} samples, which corresponds to a measurement with a total duration of 11.25 h. In the case of the larger vesicles from dialysis, 65 measurements (sample time 10 μs, No. of samples 2×10^7) were carried out. Here, the averaged data were obtained from a total of 1.3×10^9 samples, or from a measurement of 3.6 h duration. The data were analysed with the inversion algorithm CONTIN [33–35] applying the extension which takes normalisation errors into account [32,36]. Mass density distributions in terms of the hydrodynamic radius were obtained using the option that includes the model of spherical shells in the inversion algorithm. A thickness of 4.5 nm was used for the vesicle membrane. The measurements were carried out at 20°C at an angle of 90°. The viscosity and refractive index of water were used.

2.4. Incorporation of the fluorophores

The vesicle suspensions were diluted with Tris buffer (100 mM NaCl, pH 7.5) to a final concentration of 1 mM lipid. 10 μl of ethanolic stock solutions (10^{-3} M) of the dyes were added in small portions under stirring to a final dye concentration of 5×10^{-6} M. All samples were saturated with N_2.

2.5. Measurement of fluorescence decay

The determination of the time-dependent fluorescence behaviour was carried out with a commercial single photon counting apparatus of high precision (model 199 S, Edinburgh Instruments). Data were acquired between 5000 and 10000 peak counts in the temperature range 1 to 50°C. All reported decay times were averages of 10 measurements with low values of χ^2 (< 1.2). Samples of large and small vesicles were measured alternately to provide identical conditions. The excitation wavelength was 337 nm. The emission wavelengths for the AS-dyes and TNS were 430 nm and 520 nm, respectively, with an emission bandpass of 4 nm. Two further sets of sample preparations yielded identical results with all three fluorophores.

2.6. Data analysis of the fluorescence decay curves

The data were analysed using a least-squares iterative reconvolution technique as described elsewhere [37]. All data were fitted very well by a biexponential model. A triexponential decay law as well as distribution functions (Kohlrausch–Williams–Watts, Lorentz [37]) did not provide better χ^2 values. Mean decay

times τ_m were calculated as described by Lakowicz [38].

In the case of the solvent relaxation kinetics (TNS) one preexponential factor was negative, which indicates an excited state process. The lifetime τ_R with a positive preexponential factor characterizes the fluorescence of the mean relaxed state R at the red edge of the emission spectrum [1]. From the decay constant τ_{exp} of the negative term and from τ_R the solvent relaxation time τ_r was calculated for each temperature according to the equation [1]:

$$1/\tau_{exp} = 1/\tau_R + 1/\tau_r . \quad (2)$$

3. Results

3.1. Size distribution of vesicles

The mass density distributions obtained from dynamic light scattering measurements of the two samples of unilamellar phospholipid vesicles are shown in Fig. 1. The vesicles prepared from mixed lipid-cholate micelles by gel filtration have an average mass-

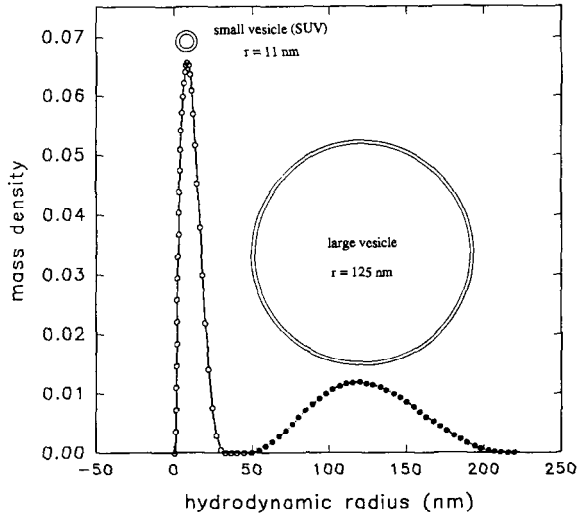

Fig. 1. Mass density distributions obtained from dynamic light scattering measurements on two samples of unilamellar phospholipid vesicles prepared from mixed-cholate micelles by gel filtration (○), and prepared from mixed lipid-octyl glucoside micelles by dialysis (●). Ordinate scale is such that the area under each peak is equal to one. The drawing scale between the small and large vesicle diameter is chosen as 1 : 10 for simplicity; the thickness corresponds to a double layer (~ 40 Å).

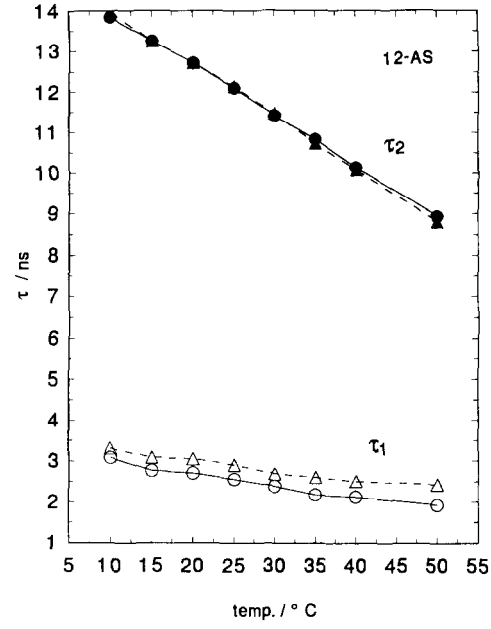

Fig. 2. Temperature dependence of the fluorescence decay times $\tau_{1,2}$ (ns) of 12-AS in large (○) and small (△) vesicles (biexponential model, $\lambda_{ex} = 337$ nm, $\lambda_{em} = 430$ nm).

weighted radius of 11 nm ($= r_m$) with a distribution width (standard deviation, Δr_m) of 2.9 nm. For the vesicles prepared from mixed lipid-octylglucoside micelles by dialysis the parameters $r_m = 125$ nm and $\Delta r_m = 31$ nm were determined.

3.2. Decay time measurements

12-(9-Anthroyloxy)stearic acid (12-AS)

The decay behaviour for all temperatures is biexponential. A monoexponential model yields only poor fits. The contributions of the two lifetime components are about 15% for the short and 85% for the long component. Within experimental error the short and long decay times are identical for large and small vesicles (Fig. 2), respectively. For both systems the decay times decrease with rising temperature. The short decay times ($\tau_1 \approx 2$–3 ns) show larger errors (up to 10%) due to their lower amplitude than the long ones ($\tau_2 \approx 10$–14 ns).

2-(9-Anthroyloxy)stearic acid (2-AS)

As for 12-AS the decay behaviour is biexponential, whereby both decay times are shorter for 2-AS. The amplitude A_2 of the longer lifetime component covers

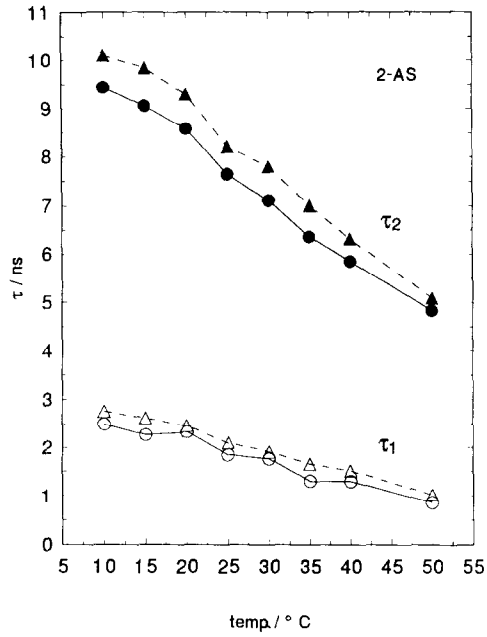

Fig. 3. Temperature dependence of the fluorescence decay times $\tau_{1,2}$ [ns] of 2-AS in large (○) and small (△) vesicles (biexponential model, $\lambda_{ex} = 337$ nm, $\lambda_{em} = 430$ nm).

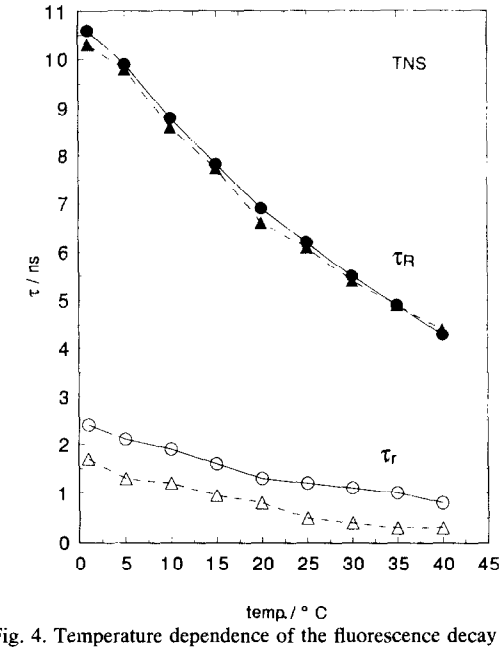

Fig. 4. Temperature dependence of the fluorescence decay time of the mean relaxed state, τ_R (ns), and of the solvent relaxation time τ_r [ns] for TNS in large (○) and small (△) vesicles (biexponential model, $\lambda_{ex} = 337$ nm, $\lambda_{em} = 520$ nm).

about 75% of the total fluorescence. Over the entire temperature range the small cholate vesicles show significantly longer decay times τ_2 than the large vesicles (Fig. 3). The same trend is observed for the mean decay times τ_m (not shown). Due to the large errors (up to 10%) the observed scatter in the short decay times τ_1 is not significant.

2-p-toluidinylnaphthalene-6-sulfonic acid (TNS)

Biexponential analysis yielded a fluorescence lifetime τ_R with a positive amplitude, decreasing from about 10 ns to less than 5 ns in the temperature range (1–40°C) (Fig. 4).

According to the model of Gonzalo and Montoro [1] this component represents the fluorescence decay of a mean relaxed state R at the red edge of the emission spectrum. For both vesicle systems the second component τ_{exp} was obtained with negative preexponential factors for all temperatures. This indicates that the relaxation from the initially excited Franck Condon state to the energy levels, which account for the red-edge fluorescence, occurs on the ns time scale. From τ_{exp} the solvent relaxation time τ_r was calculated using Equation (2). In Fig. 4 the temperature dependence of τ_R and τ_r for large and small vesicles is shown. While the decay time of the mean relaxed state τ_R is identical for large and small vesicles within experimental error, the solvent relaxation times τ_r are always faster in small vesicles than in the large ones.

In a further experiment, the long-time behaviour of TNS was determined in small vesicles at 40°C. No changes in the decay times nor in the amplitudes were detected over a measurement time of 24 h. For τ_R a constant value of 4.4 ns was obtained. The short component showed negative preexponentials at all times and yielded a constant solvent relaxation time of 0.2 ns (Fig. 5). This shows that TNS does not diffuse appreciably into the interior of the double layer.

4. Discussion

The different sizes of the two vesicle systems reflect significant differences in the membrane curvature (Fig. 1). These two types of vesicles are thus well suited as model systems for investigating curvature effects in membranes.

It is known that the fluorescent dye TNS is adsorbed at the lipid–water interface region of membranes [11–

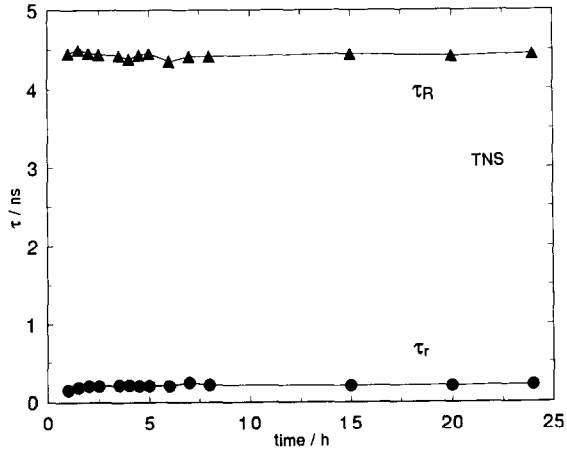

Fig. 5. Test for long-time behaviour (24 h) of the fluorescence decay times of the mean relaxed state, τ_R (ns), and of the solvent relaxation time τ_r (ns) for TNS in small vesicles (biexponential model, $\lambda_{ex} = 337$ nm, $\lambda_{em} = 520$ nm).

13], where it shows strong fluorescence. Since it does not fluoresce in aqueous solution, fluorescence of non-adsorbed molecules can be neglected. Due to its negative charge, diffusion to the inner leaflet of the bilayer should not occur significantly. In fact, the fluorescence decay behaviour ($\lambda_{em} = 520$ nm) of TNS adsorbed to the small vesicles at 40°C does not change even during 24 h. Thus for the measurement time of one sample (~ 24 h) the migration of TNS to the inner lipid–water interface can be neglected.

The quantitative analysis of the reorientation of the hydrated phospholipid headgroups, applying TNS fluorescence, was carried out using the model of Gonzalo and Montoro [1]. For the fluorescence decay curves measured at the red edge of the emission spectra this model yielded excellent fits over the entire temperature range. Although a phase transition for phosphatidylcholine does not occur in the examined temperature range, measurements were performed at nine different temperatures to show the consistency of the results, especially concerning the differences in relaxation behaviour.

As shown in Fig. 4, the fluorescence decay times τ_R of the mean relaxed state of TNS are identical within experimental error for small and large vesicles. This indicates an identical localization of TNS in both systems in spite of differences in membrane curvature. The decrease of τ_R with increasing temperature is due to an increased collision frequency of the diffusion controlled solvent quenching process in the fluid crystalline state. The average relaxation time τ_r reflects the reorientation kinetics of the fluorophore environment, induced by the dramatic increase of the fluorophore dipole moment in the excited state. In both samples the mobility of the hydrated phospholipid headgroups appears to increase with temperature, as indicated by the shortening of the solvent relaxation times. The small unilamellar vesicles, however, show a considerably faster solvent relaxation than the large ones (Fig. 4). This may be explained by a lower packing density of the headgroups at the outer surface of the highly curved membrane of the small vesicles. Hence a higher mobility of the hydrated headgroups of the smaller vesicles is expected. We are not able to distinguish between the contribution of the lipid headgroups and tightly bound water molecules to the relaxation process. Furthermore, we may be sure that the observed relaxation is not caused by bulk water molecules, since solvent relaxation in pure solvents is much faster (ps regime) and it cannot be detected with our time resolution (ns regime).

The interpretation presented is in agreement with ^{1}H-NMR studies [17], demonstrating increasing headgroup packing density with increasing vesicle size.

n-(9-anthroyloxy)stearic acids are assumed to be located at a defined depth mainly in the outer monolayer [39]. Since their lifetimes depend largely on the polarity of the environment, they have been used for detection of water penetrating into the membrane [40]. As shown by Kleinfeld et al. [8] the decay is biexponential due to two different conformers. The relaxation from the initially exited Franck Condon state (S_1^{FC}) to the state with equilibrium geometry (S_1^{EQ}) involves rotation of the carbonyl from a perpendicular orientation (relative to the plane of the anthracene ring) towards a more coplanar position [8]. Although the decay may actually occur from a continuum of intermediates during the relaxation from S_1^{FC} to S_1^{EQ} we perform the analysis in terms of two discrete components. We prefer the biexponential analysis to a distribution because the observed two lifetimes are not a result of site heterogenity of the dye (as may be the case for diphenylhexatrien (DPH) which will sample different environments along the membrane normal). 12-AS monitors the region between the 9th and 16th C-atom [41] of the outer leaflet. It does not show any significant difference in the decay behaviour in both types of vesicles; the two decay times as well as the corresponding ampli-

tudes are identical within experimental error.

2-AS is positioned between the interface and the 5th and 6th C-atom of the bilayer [41] thus probing a more polar environment than 12-AS. This accounts for shorter decay times than for 12-AS. Furthermore, 2-AS should be more sensitive to differences in the headgroup packing than 12-AS. As shown in Fig. 3, the lifetimes τ_2 of 2-AS are shorter for the larger vesicles at all examined temperatures. Two reasons may be given for the fact that only the long decay time shows a clear response to curvature. First, the uncertainty in the short lifetime values τ_1 for 2-AS (and 12-AS) may reach 10% due to the lower amplitude of this component; thus differences between small and large vesicles regarding the short decay times are within experimental error. Secondly, S_1^{FC} (contributing the short decay time) is deactivated to a large amount by the intramolecular relaxation and thus may be less sensitive to curvature effects.

As mentioned above, the fluorescence lifetimes of 2-AS in membranes depend highly on the polarity of the microenvironment. Considerations regarding the surface area ratios of inner to outer leaflet lead to the conclusion that the smaller vesicles provide more space between the lipid headgroups. Due to the high curvature of the small vesicles 2-AS is expected to be positioned somewhat deeper in the membrane in the small vesicles than in the large ones. Therefore, 2-AS will probe a more hydrophobic environment with an expected longer fluorescence decay time τ_2 in the highly curved vesicles due to less effective fluorescence quenching. This physical expectation is borne out by experiment: The lifetimes τ_2 for 2-AS in small vesicles are longer than in the large vesicles.

We conclude that the differences in lipid packing in large and small vesicles do not affect the fluorescence quenching deep inside the bilayer. However, differences in curvature play a significant role in the quenching processes of fluorophors embedded in the peripheral region of the bilayer.

Acknowledgements

We gratefully acknowledge discussions with E. Grell and thank the 'Deutsche Forschungs-gemeinschaft' and the 'Fonds der Chemischen Industrie' for partial support of this work.

References

[1] I. Gonzalo and T. Montoro, J. Phys. Chem. 89 (1985) 1608.
[2] B.R. Lentz, Chem. Phys. Lipids 50 (1989) 171.
[3] D.A. Barrow and B.R. Lentz, Biophys. J. 48 (1985) 221.
[4] F.G. Prendergast, R.P. Haugland and J.P. Callahan, Biochemistry 20 (1981) 7333.
[5] F.G. Prendergast, Period. Biol. 83 (1981) 69.
[6] J.M. Collins and W. McLean Grogan, Biochim. Biophys. Acta 1067 (1991) 171.
[7] K.R. Thulburn, in: Fluorescence probes, eds. G.S. Beddard and M.A. West (Academic Press, New York, 1981).
[8] E.D. Matayoshi and A.M. Kleinfeld, Biophys. J. 75 (1981) 215.
[9] D.R. James, J.R. Turnbull, B.D. Wagner, W.R. Ware and N.O. Petersen, Biochemistry 26 (1981) 6272.
[10] K. Brand, M. Hof and F.W. Schneider, Ber. Bunsenges. Physik. Chem. 95 (1991) 1511.
[11] R.P. De Toma, J.H. Easter and L. Brand, J. Am. Chem. Soc. 98 (1976) 5001.
[12] J.H. Easter, R.P. De Toma and L. Brand, Biochim. Biophys. Acta 508 (1978) 27.
[13] J.R. Lakowicz, R.B. Thompson and H. Cherek, Biochim. Biophys. Acta 734 (1983) 295.
[14] J.R. Lakowicz, H. Cherek, G. Laczko and E. Gratton, Biochim. Biophys. Acta 777 (1984) 183.
[15] J.R. Lakowicz, D.R. Bevan, B.P. Maliwal, H. Cherek and A. Balter, Biochemistry 22 (1983) 5714.
[16] H. Eibl and A. Blume, Biochim. Biophys. Acta 533 (1979) 476.
[17] C.G. Brouillette, J.P. Segrest, T.C. Ng and J.L. Jones, Biochemistry 21 (1982) 4569.
[18] S.F. Greenwood, F.R. Bourgeois and M.A. Rosemann, J. Biol. Chem. 261 (1986) 3670.
[19] R.E. Silversmith and G.L. Nelsestuen, Biochemistry 25 (1986) 7717.
[20] A.J. Abbott and G.L. Nelsestuen, Biochemistry 26 (1987) 7994.
[21] P.L.A. Giesen, G.M. Willems and W.T. Hermens, J. Biol. Chem. 266 (1991) 1379.
[22] B.R. Lentz, G.F. McIntyre, D.J. Parks, J.C. Yates and D. Massenburg, Biochemistry 31 (1992) 2643.
[23] P.L.A. Giesen, Biochim. Biophys. Acta 1147 (1993) 125.
[24] J.R. Lakowicz, J. Biochem. Biophys. Methods 2 (1980) 81.
[25] T. Parasassi, F. Conti and E. Gratton, Cell. Mol. Biol. 32 (1986) 99.
[26] M. Maroncelli and G.R. Fleming, J. Chem. Phys. 86 (1987) 6221.
[27] J. Brunner, P. Skrabal and H. Hauser, Biochim. Biophys. Acta 455 (1976) 322.
[28] L.T. Mimms, G. Zampighi, Y. Nozaki, C. Tanford and J.A. Reynolds, Biochemistry 20 (1981) 833.

[29] W.S. Singleton, M.S. Gray, M.L. Brown and J.C. White, J. Am. Oil Chem. Soc. 42 (1965) 53.
[30] L.D. Mayer, M.J. Hope, P.R. Cullis and A.S. Janoff, Biochim. Biophys. Acta 817 (1985) 193.
[31] G.R. Bartlett, J. Biol. Chem. 234 (1959) 466.
[32] H. Ruf, E. Grell and E.H.K. Stelzer, Europ. Biophys. J. 21 (1992) 21.
[33] S.W. Provencher, J. Hendrix, L. De Maeyer and N. Paulussen, J. Chem. Phys. 69 (1978) 4273.
[34] S.W. Provencher, Comput. Phys. Commun. 27 (1982) 213.
[35] S.W. Provencher, Comput. Phys. Commun. 27 (1982) 229.
[36] H. Ruf, Biophys. J. 56 (1989) 67.
[37] M. Hof, J. Schleicher and F.W. Schneider, Ber. Bunsenges. Physik. Chem. 93 (1989) 1377.
[38] J.R. Lakowicz, Principles of fluorescence spectroscopy, (Plenum Press, New York, 1983).
[39] N. Shaklai, J. Yguerabide and H.M. Ranney, Biochemistry 16 (1977) 5585.
[40] K. Brand, Ph.D. Thesis, University of Würzburg (1993).
[41] G.B. Zavoico, L. Chandler and H. Kutchai, Biochim. Biophys. Acta 812 (1985) 299.